# USING A FATIGUE DATA EDITING APPROACH FOR ANALYSING CYCLE SEQUENCE EFFECTS IN VARIABLE AMPLITUDE ROAD LOADINGS

**S. Abdullah[1] and J.C. Choi[2]**

*[1]Department of Mechanical and Materials Engineering, Universiti Kebangsaan Malaysia, 43600 UKM Bangi, Selangor*

*[2]Hyundai Motor Company, South Korea*

*E-mail: shahrum@eng.ukm.my*

## ABSTRACT

*This paper presents the analysis of cycle sequence effects using variable amplitude (VA) fatigue loadings extracted from a wavelet-based fatigue data editing algorithm, known as Wavelet Bump Extraction (WBE). This algorithm was used to produce a shortened mission signal by extracting fatigue damaging events from the original signal. In relation to the fatigue life prediction, current industrial practice uses the Palmgren-Miner linear damage rule which lacks load interaction accountability in VA loadings. Considering the importance of cycle sequence effects in VA loadings, a suitable fatigue life prediction approach was identified, i.e. the Effective Strain Damage (ESD) model. In this study, the cycle sequence effects were analytically and experimentally analysed using VA fatigue loadings. Uniaxial fatigue tests of the WBE extracted loadings were performed and the results were compared with predicted results using four strain-life models, i.e. Coffin-Manson, Morrow, Smith-Watson-Topper (SWT) and ESD. The smallest and acceptable difference of about 19% between the experiment and prediction was found using the ESD model. Finally, to note that it is important to retain the original cycle sequence in order to properly determine fatigue life under VA loadings.*

***Keywords:*** *Fatigue, Fatigue Data Editing, The ESD Model, Variable Amplitude, WBE*

## 1. INTRODUCTION

Fatigue life prediction is important in the design process of vehicle structural components, with the essential input variable for fatigue is the load history. Practically, automobile manufacturers go to great lengths to instrument vehicles and subject them to a variety of driving conditions. By necessity, vehicle development requires accelerated fatigue testing and this is often accomplished by correlating test tracks with public road data. Both roads and test tracks generate variable amplitude (VA) load time histories. Loads that are predicted to do little or no damage can be eliminated and large amplitude cycles are retained. The process can be performed using a wavelet-based fatigue data editing, known as Wavelet Bump Extraction (WBE) algorithm, which was developed by Abdullah et al. [1-3].

The situation where the order of loading affects the fatigue life is called a sequence effect, which is related to both crack initiation and crack propagation stages [4], and overload (OL)/ underload (UL) occurrence in VA loadings [5,6]. Extensive studies of the OL and UL effects on the metal fatigue have been previously performed [5,7,8]. For these cases, when overloads were inserted in the small cycle or below the material fatigue limit, the small cycles following the overloads contributed to the fatigue damage accumulation. Considering the importance of sequence effects and the limitation in the linear damage rule to predict fatigue damage under VA loadings [9], therefore a suitable approach should be applied.

In this paper the cycle sequence effects are analysed using the VA loadings extracted from the WBE algorithm. The original VA loading chosen for this study, which was the input for the WBE algorithm, was measured on the lower suspension arm of an automobile when travelling over a pavé test track surface. The experimental study was performed by applying uniaxil fatigue tests on to a simple specimen using these WBE extracted loadings. The analytical fatigue lives using four strain-life models were then compared to experimental findings in order to observe the load interaction effects in fatigue damage prediction. Based on the literature search by the authors, no studies have been performed in the analysis of cycle sequence effects using loadings extracted from fatigue data editing algorithms. The results obtained from this paper can then be used for the validation process of the effectiveness of the WBE algorithm.

## 2. FATIGUE LIFE PREDICTONS

Current industrial practice for fatigue life prediction is to use the Palmgren-Miner [10,11] linear damage rule. This rule is normally applied with strain-life fatigue damage models for analysing shorter fatigue life problems [9]. The strain-life fatigue life behaviour considers plastic deformation that occurs at the localised region where fatigue cracks begin with the influence of a mean stress. The first strain-life model is the Coffin-Manson relationship and is defined as [12,13]

$$\varepsilon_a = \frac{\sigma_f'}{E}(2N_f)^b + \varepsilon_f'(2N_f)^c \qquad (1)$$

where $\sigma_a$ is the stress amplitude, $\sigma_f'$ is the fatigue strength coefficient, $E$ is the modulus of elasticity, $N_f$ is the number of cycles to failure, b is the fatigue strength exponent, $\varepsilon_f'$ is the fatigue ductility coefficient and $c$ is the fatigue ductility component.

Some of the realistic service situations involve non-zero mean stresses. Two mean stress effect models are used in the

strain-life fatigue damage analysis, i.e. Morrow and Smith-Watson-Topper (SWT) strain-life models. Mathematically, the Morrow's model is defined by [14]

$$\varepsilon_a = \frac{\sigma_f'}{E}\left(1 - \frac{\sigma_m}{\sigma_f'}\right)(2N_f)^b + \varepsilon_f'(2N_f)^c \quad (2)$$

where and $\sigma_m$ is the mean stress. The Smith-Watson-Topper (SWT) strain-life model is mathematically defined as [15]

$$\sigma_{max}\varepsilon_a = \frac{(\sigma_f')^2}{E}(2N_f)^{2b} + \sigma_f'\varepsilon_f'(2N_f)^{b+c} \quad (3)$$

where and $\sigma_{max}$ is the maximum stress.

There are some limitations were found during the implementation of the Palmgren-Miner linear damage rule. The fatigue damage is accurately calculated for constant amplitude (CA) loadings, but it may lead to the erroneous prediction for VA loadings [9]. It is because the Palmgren-Miner linear damage rule assumes no load sequence effect and lacks load interaction accountability. Considering the importance of sequence effects in VA loadings, therefore, a suitable approach was identified.

The problem of performing fatigue life predictions for uniaxial VA fatigue loadings has been discussed by Fatemi and Yang [16]. It has been noted that the experimental fatigue lives of components subjected to VA loadings can be well below the fatigue life predicted using CA fatigue tests [17]. The reason for these fatigue life differences is that a VA loading contains a mixture of large and small amplitude cycles which contribute to the cycle sequence effects. The large load cycles in a VA loading affect the increment of the effective stress for the subsequent smaller cycles. Hence, the crack growth rate for the smaller cycles is increased, and even small cycles below the CA fatigue limit can cause a significant amount of fatigue damage [18].

Several investigators have proposed methods for improving the fatigue life prediction for components subjected to VA loadings. Models have been derived using random vibration theory [19], using non-linear damage summation [20], and by adopting a fracture mechanics approach [21]. Methods of modifying the stress-life and strain-life approaches have been suggested in order to predict the fatigue life of the metal structures and automobile components exposed to VA loadings [17].

Although such models have provided improved fatigue life predictions under VA loadings compared to the CA linear damage methods under specific conditions, they have proved difficult to incorporate in fatigue life prediction programmes for general use. Considering the limitations observed in the fatigue life predictions determined for VA loadings, the use of a simple linear damage model such as the Palmgren-Miner rule has been found to be unsuitable. Therefore, a fatigue damage model for use with VA loadings was developed by DuQuesnay et al. [5], called the Effective Strain Damage (ESD) strain-life model.

The ESD model was developed based on crack detection criteria and it uses the effective strain range as the damage parameter. It has been shown to work well for a wide range of materials, load spectra, component geometries, strain magnitudes and mean-strain effects [5,6]. Using this model, the fatigue damage is analysed based on the assumption of short crack growth, since the crack length at failure is usually less than a few millimetres. The ESD model is mathematically defined as

$$E\Delta\varepsilon^* = A(N_f)^B \quad (4)$$

where $E$ is the elastic modulus of the material, $\Delta\varepsilon^*$ is a net effective strain range for a closed hysteresis loop that is related to fatigue crack growth. $A$ and $B$ are the material constants, and $N_f$ is the number of cycles to failure. The magnitude of $E\Delta\varepsilon^*$ for a given cycle is a function of crack-opening stress, $S_{op}$, level and it is dependant on the prior stress and strain magnitudes in the loading history.

The expression of $E\Delta\varepsilon^*$ can be expanded to

$$E\Delta\varepsilon^* = E(\varepsilon_{max} - \varepsilon_{op}) - E\varepsilon_i \quad (5)$$

where $\varepsilon_{max}$ and $\varepsilon_{op}$ is the maximum strain and the crack-opening strain of the particular cycle, respectively. $\varepsilon_i$ is the intrinsic fatigue limit strain range under the VA loading condition. In order to consider the cycle sequence effects in the fatigue life calculation, a decay parameter, $m$, is used to define the change in a crack-opening stress between two adjacent cycles. $\Delta S_{op}$ was first defined as [18]

$$\Delta S_{op} = m(S_{ss} - S_{cu}) \quad (6)$$

where $S_{cu}$ is the current opening stress and $S_{ss}$ is the steady-state opening stress. $S_{cu}$ is defined as the $S_{op}$ value of the previous cycle. $S_{ss}$ is defined as

$$S_{ss} = \alpha S_{max}\left(1 - \left(\frac{S_{max}}{S_y}\right)^2\right) + \beta S_{min} \quad (7)$$

where $\alpha$ and $\beta$ are the material constants, $S_{max}$ is the maximum stress of the previous largest cycle in the time history, $S_{min}$ is the minimum stress of the previous largest cycle and $S_y$ is the cyclic yield stress.

## 3. WAVELET BUMP EXTTRACTION (WBE)

### A. APPROACHES IN WBE

In durability test of automobiles, load histories under particular driving conditions are often collected [22]. These experimental loadings exhibit time-varying, or nonstationary characteristics, which provide a challenge in the analysis. The frequency domain of the time series was performed using the Fourier transform, but it is not suitable to analyse nonstationary signals. It is due to inability of the Fourier transform to provide information of the spectrum changes with respect to time. However, this problem can be solved using the wavelet transform. A wavelet is a function in the time-scale domain and a significance tool for presenting local features of a signal. The wavelet transform gives a separation of components of a signal that overlap in both time and frequency and produce a more accurate local description of the signal characteristics [23].

In this research, the Wavelet Bump Extraction (WBE) algorithm was designed [1-3] as a tool for accelerated fatigue

tests. Using WBE, high amplitude or bump segments were extracted with the retention of the original load cycle sequences. WBE has three main stages, as illustrated in Figure 1: the wavelet decomposition process, the identification and extraction of the fatigue damaging events, and the production of a mission signal. WBE uses the orthogonal wavelet transform by means of the 12th order Daubechies wavelets [24] which were chosen as the basis functions. Each wavelet level describes the time behaviour of the signal in a frequency band.

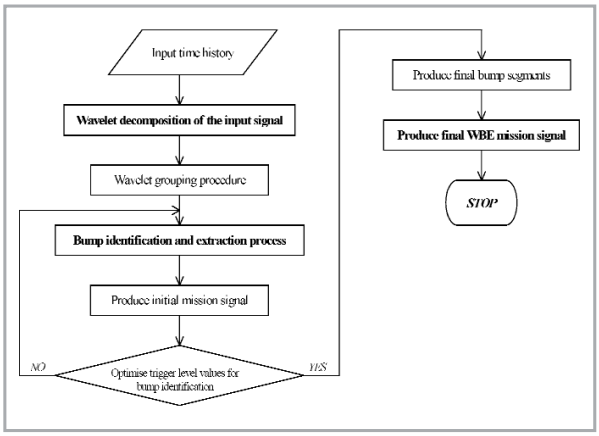


***Figure 1: A flowchart of the Wavelet Bump Extraction (WBE) algorithm***

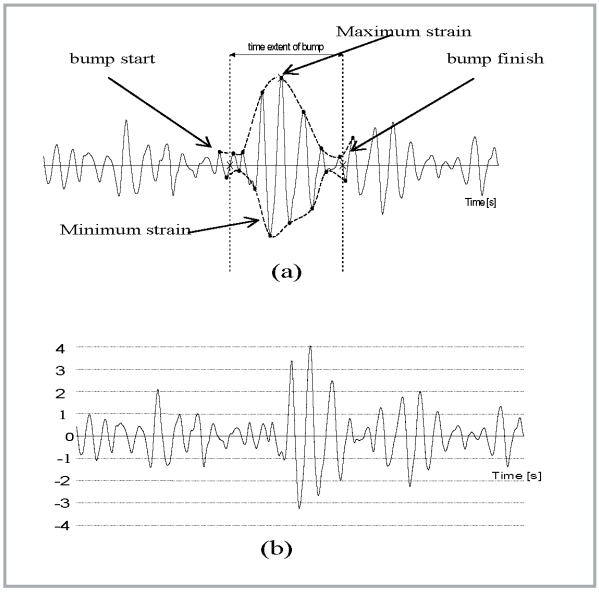


***Figure 2: (a) decay enveloping of a bump, (b) possible trigger level values***

Using the WBE algorithm, fatigue damaging events are identified in wavelet groups. A wavelet grouping stage permits the user to cluster wavelet levels into a single region of significant signal vibrational energy. A bump, which is an oscillatory transient with a monotonic decay envelope either side of a peak value (Figure 2a), is identified in each wavelet group by means of an automatic trigger level (Figure 2b). At program launch the user specifies the maximum acceptable percentage difference (±10%) between the root-mean-square (r.m.s.) and kurtosis values of the original signal and the mission signal. The r.m.s. is used to quantify the overall energy content of the oscillatory signal, and the kurtosis is used as a measure of non-gaussianity since it is highly sensitive to outlying data among the instantaneous values. The r.m.s. and kurtosis of the mission signal are then compared to those of the original signal. If the statistics exceed the required difference, the trigger levels are reduced by a user specified step until the statistical values achieve the user-specified tolerance.

After all the bumps are identified in the wavelet groups, a method of searching the bump start and finish points from the original time history has been introduced. If a bump event is found in any of the wavelet groups, a block of data covering the time frame of the bump feature is extracted from the original data set. This data selection strategy, which is shown in Figure 3, retains the amplitude and phase relationships of the original signal. The final process in the WBE processing is to produce a shortened mission signal, in which the bump segments extracted from the original time history are joined together, as illustrated in Figure 4. This strategy produces a mission time history with an equivalent signal statistics and fatigue damage potential of the original loading.

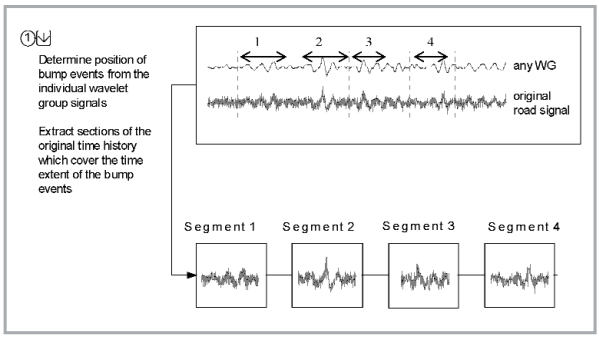


***Figure 3: Production of WBE bump segments***

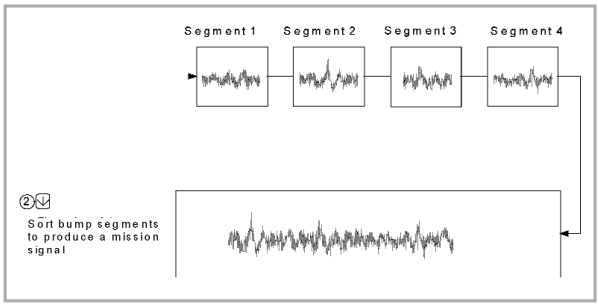


***Figure 4: Generation of a WBE signal from a combination of bump segments***

## B. APPLICATION OF WBE USING VARIABLE AMPLITUDE LOADINGS

The effectiveness of the WBE algorithm in the extraction of appropriate bump segments, which discussed in Abdullah *et al.* [1-3], was performed using a synthetic signal containing a mixture of high sinusoidal amplitude in the low amplitude background. As regard to this paper, however, an experimental measured road load data is used as an input data for the WBE processing. Using WBE, this bump segments which might produce higher fatigue damage are extracted. These segments are

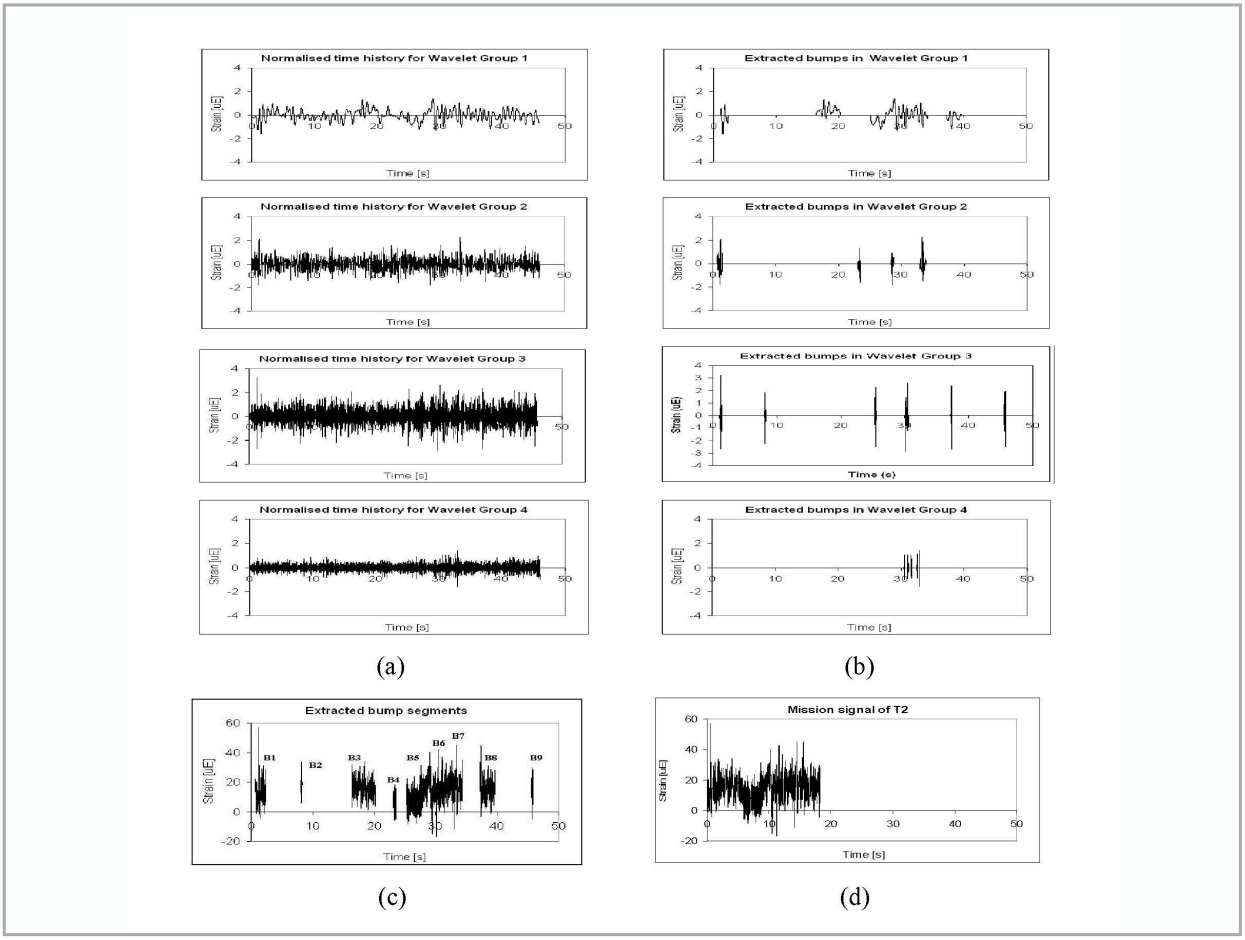


***Figure 6: Time history plots for: (a) The wavelet groups in normalized scale, (b) Location of the individual bumps in the respective wavelet group, (c) Bump segments extracted at the original time positions where B1 to B9 denoted as the number of bump segment, (d) The WBE mission signal***

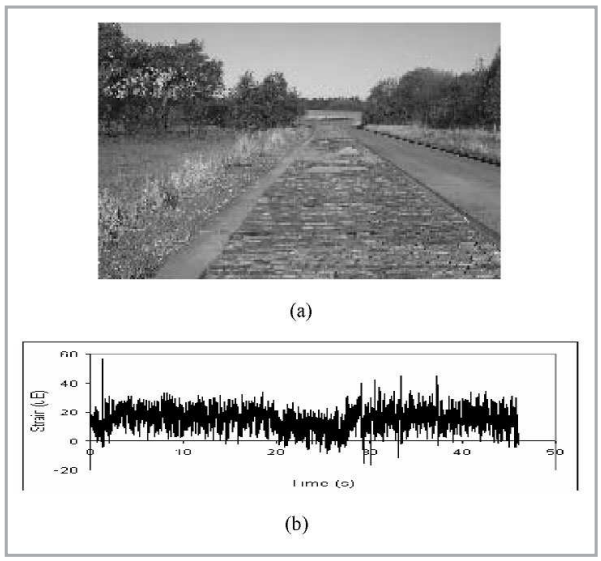


***Figure 5: (a) Pave test track used to measure road load, (b) Experimetally measured VA laoding***

then used for the uniaxial fatigue loadings in order to determine their fatigue life in practice. The fatigue lives of these segments are also predicted using the available strain-life fatigue damage model. The findings can then be compared to those obtained in the experiment for the fatigue cycle sequence analysis.

A variable amplitide (VA) strain loading was measured on a van suspension arm while driving over a pavé test track surface at 34 km/hr, the signal of which was provided by Leyland Technical Centre (LTC), United Kingdom. Figure 5a presents a photograph of the pavé surface used during the tests. The suspension arm pavé test data set, as the time history plot is shown in Figure 5b, was chosen because it contained many small amplitude, high frequency, bumps in the signal background. This signal exhibits a slight change in mean of the whole signal with a little low frequency content. The signal was sampled for 23,000 discrete points at a sampling rate of 500 Hz, producing the length of the entire signal is 46 seconds.

Using the WBE algorithm, the signal was decomposed into 12 wavelet levels and the levels were then grouped into four wavelet groups. The wavelet group time histories are shown in Figure 6a, exhibiting different frequency data distribution for each wavelet group, i.e. low frequency for Wavelet Group 1 and high frequency for Wavelet Group 2. Bumps were extracted at ±10% r.m.s. and kurtosis difference between the original and mission signals. Figure 6b shows the high amplitude events which were identified in each wavelet group.

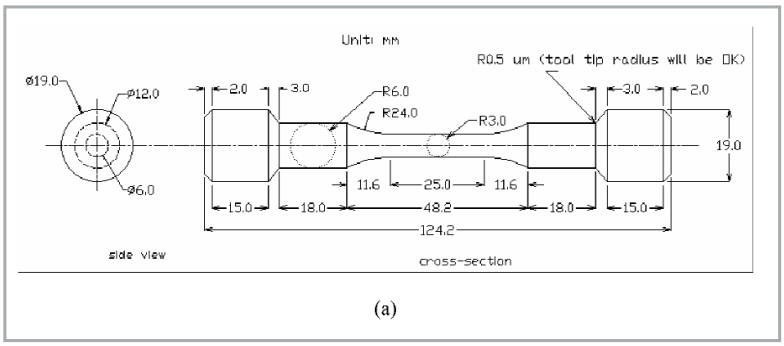


(a)

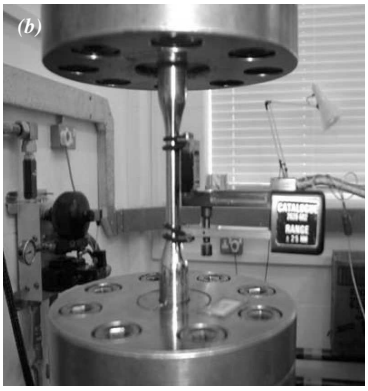


***Figure 7: (a) The geometry of a smooth specimen - all in the unit of mm unless specified, (b) A specimen at the servo-hydraulic machine with a 25-mm extensometer***

***Table 1: Mechanical properties of BS 080A42 steel [3]***

| Monotonic mechanical properties | | Cyclic mechanical properties | |
|---|---|---|---|
| Ultimate tensile strength, [MPa] | 624 | Fatigue strength coefficient, $\sigma'_f$ [MPa] | 1505 |
| Modulus of elasticity, $E$ [GPa] | 210 | Fatigue strength exponent, $b$ | -0.144 |
| Static yield stress [MPa] | 342 | Fatigue ductility coefficient, $\varepsilon'_f$ | 0.176 |
| Area reduction, [%] | 51.9 | Fatigue ductility exponent, $c$ | -0.400 |
| Elongation [%] | 28.4 | Material constant $A$ [GPa] in Eq. (4) | 119 |
| | | Material constant $B$ in Eq. (4) | -0.5 |
| | | Decay parameter $m$ in Eq. (6) | 0.002 |
| | | Material constant $\alpha$ in Eq. (7) | 0.55 |
| | | Material constant $\beta$ in Eq. (7) | 0.23 |

The extracted bump segments are displayed in Figure 6c, showing nine bump segments which were located at their original time position. In order to produce the WBE mission signal, these extracted individual bump segments were assembled as shown in Figure 6d. In terms of time compression, the length of the mission signal is 18.8 seconds and 40.9% of the original signal.

## IV. UNIAXIAL FATIGUE TEST USING ROAD LOADINGS AND RESULTS

The material chosen for the test sample was BS 080A42 steel, which is often used in the suspension components of passenger cars. Smooth gauge specimens were manufactured as a cylindrical bar as the geometry and dimensions is shown in Figure 7a. The specimens were hand-polished with 60-1000 grades of silicone carbide abrasive papers and finished with 6-mm diamond compound in order to produce an hourglass profile. A servo-hydraulic test machine was used in displacement control mode for all tests. A strain-life curve of BS 080A42 steel, which was shown in Fig. 8, was obtained from constant amplitude (CA) fatigue tests at nine difference strain amplitudes [3]. Using the CA fatigue test data and a tensile test data [25], the mechanical properties is presented in Table 1. The cyclic mechanical properties were obtained using CA fatigue test data based on Equation (1) and Equation (4) for the CA fatigue damage models and the ESD model, respectively.

In this study, laboratory uniaxial VA fatigue tests were performed using ten WBE extracted VA loadings. They were nine extracted bump segment loadings (Figure 6c) and one mission signal (Figure 6d). The purpose of these fatigue tests is to observe the fatigue lives produced by the actual original sequence of VA loadings, so that the original fatigue cycle sequence effects can be observed. Figure 9 presents the experimental fatigue lives of the ten extracted WBE VA loadings obtained using the smooth specimens of BS 080A42 steels, which the fatigue life values are tabulated in Table 2.

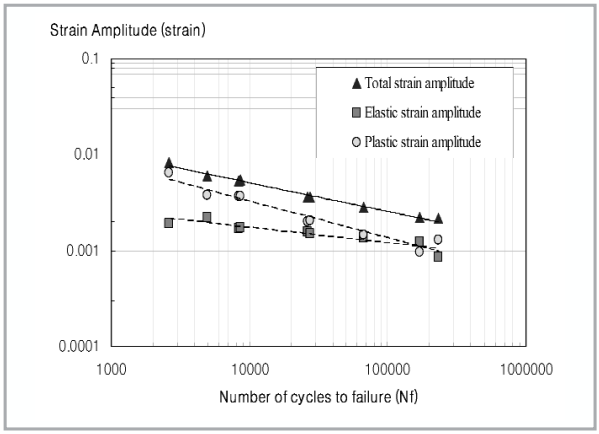


***Figure 8: Experimental strain-life curve of BS 080A42 steel [3]***

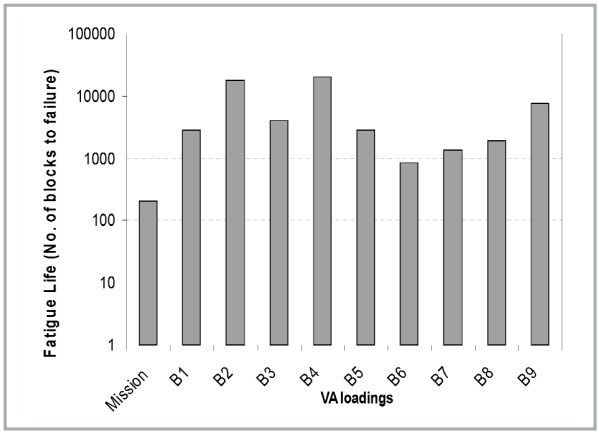


***Figure 9: Experimental fatigue lives of smooth specimens using ten VA loadings***

## V. DISCUSSIONS

In this paper, strain-life fatigue damage models were used for the fatigue life predictions and the prediction results were then compared to the experimental results. The main reason of using the strain-life models because of its suitability in analysing ductile materials at relatively short fatigue lives. This approach is also used where a little plasticity is acceptable at long fatigue lives. Accordingly, strain-life approaches are comprehensive and

can be used in place of stress-life approaches. It is common that the service loadings of machines and vehicles is evaluated using a strain-life fatigue damage approach [26,27]. Generally, the strain-life fatigue models relate the plastic deformation that occurs at a localised region where fatigue cracks begin to the durability of the structure.

Four strain-life models are discussed in this section, i.e. the Coffin-Manson relationship, Morrow and Smith-Watson-Topper (SWT) mean stress correction equations, and the ESD model. The first three are suitable for predicting fatigue lives under constant amplitude (CA) fatigue loadings [9]. However, these three models are not suitable for variable amplitude (VA) loadings as the cycle sequence effects are not accounted for. Despite this, these CA-based fatigue damage models are often used for VA problems in practice. To properly treat VA loading histories, the ESD strain-life model was developed [5] for fatigue life prediction of VA loadings and this model was based on life-to-crack detection by treating the effective strain range as the damage parameter. In this model, the fatigue damage is analysed based on short crack growth concepts to incorporate retardation by changing crack closure levels.

In order to calculate fatigue lives of VA loadings using the ESD model, the fatigue cycles should be reconstructed based on the original position in the time history. This reconstruction procedure is required in order to retain the original load cycle sequences present in the original VA loading. Cycle reconstruction is not required for CA loadings, since the cycle sequences are not affected in the fatigue life prediction using this type of loading. The fatigue cycle reconstruction consists of converting a time history into a series of peak-valley reversals. These reversals were then rainflow counted [28] in order to extract fatigue cycles. The cycles were then sorted based on the peak-valley history in order to produce a similar pattern to the original load sequences. For example, a reconstructed cycle history is shown in Figure 10 for the first bump segment (B1) of the signal.

Table 2 shows the fatigue lives of the ten VA loadings calculated using four strain-life models, which were tabulated together with the experimental fatigue lives. The experimental uniaxial fatigue lives in Table 2 were compared between the prediction and experimental values. Figure 11 shows the correlation of fatigue lives between experiment and all four strain-life models. Each data point represents a loading condition in Table 2. In this figure the correlated fatigue lives between the ESD model and experiments were distributed around the 1:1 line and within the range of ± a factor of 2. However, the correlation points which were produced from the data of the three other strain-life models (Coffin-Manson, Morrow and SWT) were located outside the range of ± a factor of 2. The related findings obtained from this figure suggested that the ESD model had the closest agreement between the predicted fatigue life and the experimental fatigue life.

Numerically, the comparison between fatigue lives determined using the four strain-life models and the experimental findings are tabulated in Table 3. The table shows the difference (in percent) between the predicted value of a particular strain-life model and the experimental value for a particular bump segment. Then, the differences for the same strain-life model are averaged in order to obtain a single value for comparison purposes. The results in Table 3 show that the difference between the SWT model and the experimental results gave the highest value at 575%, followed by the Coffin-Manson model and the Morrow model at 323% for both. However, the smallest average difference between the prediction and the experimental values was found to be at 19%, when using the ESD model.

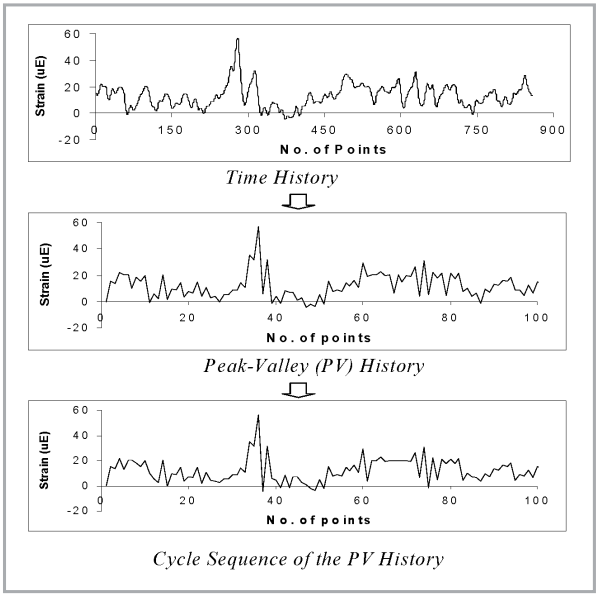


***Figure 10: Time history reconstruction for the first bump segment (B1) of the signal***

***Table 2: Fatigue lives of the bump segments and the WBE mission signal obtained using four strain-life models and determined from the uniaxial fatigue tests***

four strain-life models and determined from the uniaxial fatigue tests.

| Segment | Fatigue Life [Number of blocks to failure] | | | | |
|---|---|---|---|---|---|
| | Experiment | Coffin-Manson | Morrow | SWT | ESD |
| B1 | 2831 | 5964 | 5952 | 10462 | 1968 |
| B2 | 17880 | 97000 | 97087 | 114000 | 19523 |
| B3 | 3996 | 14008 | 14006 | 17720 | 2400 |
| B4 | 20084 | 96400 | 96154 | 163000 | 25586 |
| B5 | 2792 | 13708 | 13699 | 24566 | 2714 |
| B6 | 843 | 3428 | 3425 | 6070 | 927 |
| B7 | 1366 | 6216 | 6211 | 10409 | 1536 |
| B8 | 1942 | 9370 | 9346 | 14783 | 2206 |
| B9 | 7500 | 35667 | 35714 | 55200 | 8181 |
| *MS | 319 | 1057 | 1092 | 2013 | 204 |

*MS denoted as the WBE mission signal.

In a separate analysis, Table 4 shows the difference in total fatigue damage of the bump segments when comparing the prediction results of the strain-life models and the experiments. Similar to the data in Table 3, the SWT model produced the highest difference with respect to the experiment, which was found at 85%. It was followed by the Coffin-Manson and Morrow models, at 76% and 75%, respectively. However, the ESD model produced the smallest difference value at 2%. Using the ESD model, the lowest difference in fatigue life prediction was found as shown in Table 3 and Table 4. Since the ESD model accounts for mean stress and cycle sequence effects during the fatigue life calculation [5,6,29], high correlations were to be expected. The comparison of the experimental and analytical results obtained for the T4 bump segments suggested that the ESD model provided more

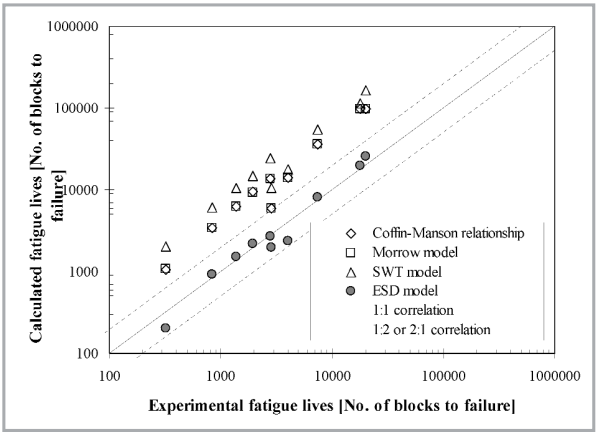


***Figure 11: Fatigue life correlations between the prediction and experiment using ten WBE loadings***

***Table 3: Fatigue life differences between prediction and experiment for ten WBE loadings***

| Signal Name | Fatigue Life Differences [%] | | | |
|---|---|---|---|---|
| | Coffin-Manson vs. Experiment | Morrow vs. Experiment | SWT vs. Experiment | ESD vs. Experiment |
| B1 | 111 | 110 | 270 | 30 |
| B2 | 443 | 443 | 538 | 9 |
| B3 | 251 | 251 | 343 | 40 |
| B4 | 380 | 379 | 712 | 27 |
| B5 | 391 | 391 | 780 | 3 |
| B6 | 307 | 306 | 620 | 10 |
| B7 | 355 | 355 | 662 | 12 |
| B8 | 382 | 381 | 661 | 14 |
| B9 | 376 | 376 | 636 | 9 |
| *MS | 231 | 242 | 531 | 36 |
| *Average* | 323 | 323 | 575 | 19 |

1. *MS denoted as the WBE mission signal.
2. Fatigue life [$N_f$] difference =absolute $\{[N_{f\ predicted} - N_{f\ experiment}]/ N_{f\ experiment}\}$ x 100%

***Table 4: Comparison of total damage accumulated for all bump segments***

| | Fatigue Life Differences [%] | | | |
|---|---|---|---|---|
| | Coffin-Manson vs. Experiment | Morrow vs. Experiment | SWT vs. Experiment | ESD vs. Experiment |
| TOTAL | 76 | 75 | 85 | 2 |

*Note: Fatigue life [$N_f$] difference =absolute $\{[N_{f\ predicted} - N_{f\ experiment}]/ N_{f\ experiment}\}$ x 100%*

accurate fatigue life predictions for VA fatigue loadings than the three other strain-life models that were considered. Since the smallest difference between the prediction and experimental fatigue lives were obtained when using the ESD model, it was showing that ESD is the most suitable strain-life fatigue damage model for VA loadings.

## V. CONCLUSIONS

The paper had discussed on the analysis of fatigue cycle sequence effects in the wavelet-based fatigue data editing algorithm, called Wavelet Bump Extraction (WBE). Several concluding remarks are highlighted based on the findings of this research:

1. WBE is a wavelet-based algorithm that can be used for fatigue data editing of variable amplitude fatigue loadings (VA) for the purpose of accelerated fatigue tests.
2. Bump segments were extracted at the ±10% r.m.s. and kurtosis difference between the mission and original signals, retaining the vibrational signal energy and fatigue damage.
3. A close agreement was obtained between the Effective Strain Damage (ESD) model and experiments, where the correlation points were distributed around the 1:1 correlation line. Hence, it is suggested that ESD is a suitable strain-life fatigue damage model accounting for the cycle sequence effects.
4. The average fatigue life difference between the ESD model and experiment was 19%, which is the smallest as compared to the other models.
5. The combination of WBE and ESD provide a novel wavelet-based fatigue data editing technique that accurately extracts the most fatigue damaging events (bump segments) and which preserves the original load cycle sequence within the fatigue loadings.

## ACKNOWLEDGEMENTS

The authors wish to express their gratitude to Universiti Kebangsaan Malaysia (Malaysia), Hyundai Motor Company (South Korea), The University Of Sheffield (United Kingdom) and Leyland Technical Centre (United Kingdom) for all the supports given for these works. ■

## REFERENCES

[1] S. Abdullah, J. R. Yates and J. A. Giacomin, Wavelet Bump Extraction (WBE) algorithm for the analysis of fatigue damage, *Proc of the 5th Int Conf on Low Cycle Fatigue (LCF5)*, Berlin, Germany, 9-11th September, pp. 445-450, 2003.

[2] S. Abdullah, J. R. Yates and J. A. Giacomin, A mission synthesis algorithm for editing variable amplitude fatigue signals, in *Integrity for Life: Structural Integrity Assessment for Life Cycle Management*, edited by Flewitt, P.E.J. et al., EMAS Publishing, Manchester UK, pp. 279-286, 2004.

[3] S. Abdullah, J. C. Choi, J. A. Giacomin and J. R. Yates, Bump extraction algorithm for variable amplitude fatigue loadings. *Int. J. Fatigue*, 2006 (in press).

[4] H. O. Fuchs and R. I. Stephens, *Metal Fatigue in Engineering*, John Wiley and Sons, New York, 1980.

[5] D. L. DuQuesnay, M. A. Pompetzki and T. H. Topper, Fatigue life prediction for variable amplitude strain histories, *SAE Transactions (SAE930400)*, Society of Automotive Engineers (SAE), Vol. 102, No. 5, pp. 455-465, 1993.

[6] T. H. Topper and T. S. Lam, Effective strain-fatigue life data for variable amplitude loading, *Int. J. Fatigue*, Vol. 19, No. Supp. No.1, pp. S137-S143, 1997.

[7] M. Hawkyard, B. E. Powell, I. Hussey and L. Grabowski, Fatigue crack growth under the conjoint action of major and minor stress cycles, *Fatigue Fract. Engng. Mater. Struct*, Vol. 19, No. 2-3, pp. 217-227, 1996.

[8] J. J. F. Bonnen and T. H. Topper, The effect of bending overloads on torsional fatigue in normalised 1045 steel, *Int. J. Fatigue,* Vol. 21, pp. 23-33, 1999.

[9] N. E. Dowling, *Behaviour of Materials: Engineering Methods for Deformation, Fracture and Fatigue*, Second Edition, Prentice Hall, New Jersey, 1999.

[10] A. Palmgren, Die Lebensdauer von Kugellagern, *Verfahrenstechinik*, Berlin, Vol. 68, pp. 339-341, 1924.

[11] M. A. Miner, Cumulative damage in fatigue, *Journal of Applied Mechanics*, Vol. 67, pp. A159-A164, 1945.

[12] L. F. Coffin, A study of the effect of cyclic thermal stresses on a ductile metals, *Transactions of ASME,* Vol. 79, pp. 931-950, 1954.

[13] [13] S. S. Manson, Fatigue: a complex subject – some simple approximation, *Experimental Mechanics*, Vol. 5, pp. 193-226, 1965.

[14] J. D. Morrow, *Fatigue Properties of Metal Fatigue Design Handbook*, Society of Automotive Engineers, 1968.

[15] K. N. Smith, P. Watson and T. H. Topper, A stress-strain function for the fatigue of metals, *Journal of Materials,* JMLSA, Vol. 5, No. 4, pp. 767-778, 1970.

[16] A. Fatemi and L. Yang, Cumulative fatigue damage and life prediction theories: a survey of the state of the art for homogeneous materials, *Int. J. Fatigue*, Vol. 20, No. 1, pp. 9-34, 1998.

[17] X. Yan, T. S. Cordes, J. H. Vogel and P. M. Didinger, A property fitting approach for improved estimates of small cycle fatigue damage, *SAE Transactions (SAE920665)*, Society of Automotive Engineers (SAE), Philadelphia USA, 1992.

[18] M. Vormwald and T. Seeger, The consequences of short crack closure on fatigue crack growth under variable amplitude loading, *Fatigue Fract. Eng. Mater. Struct.,* Vol. 14, No. 3, pp. 205-225, 1991.

[19] H. Y. Liou, W. F. Wu and C. S. Shin, A modified for the estimation of fatigue life derived from random vibration theory, *Probabilistic Engineering Mechanics,* Vol. 14, pp. 281-288, 1999.

[20] S. M. Marco and W. L. Starkey, A concept of fatigue damage, *Transaction of the ASME*, Vol. 76, pp. 627-632, 1954.

[21] O. E. Wheeler, Spectrum loading and Crack Growth, *J. Basic Eng., Trans. ASME*, Vol. D94, No. 1, pp. 181-186, 1972.

[22] E. S. Palma and M. G. M. Martins, Durability test analysis in a passenger vehicle, *Proceedings of the 12th International Conference on Experimental Mechanics (ICEM12)*, Bari, Italy, 29th August – 2nd September, paper no. 237, 2004.

[23] D. E. Newland, *An Introduction to Random Vibrations Spectral and Wavelet Analysis*, 3rd Edition, Longman Scientific and Technical, New York, 1993.

[24] I. Daubechies, *Ten Lectures on Wavelets,* SIAM, Philadelphia, 1992.

[25] J. C. Choi, *Fatigue Evaluation for the Wavelet Bump Extraction (WBE) Algorithm*, MPhil Thesis, The University of Sheffield, United Kingdom, 2004.

[26] A. Conle and R. Landgraf, A fatigue analysis program for ground vehicle components, *Proceedings of International Conference on Digital Techniques in Fatigue*, London, pp. 1-28, 1983.

[27] F. A. Conle and C. C. Chu, Fatigue analysis and the local stress-strain approach in complex vehicular structures, *Int. J. Fatigue*, Vol. 19, Supp. No. 1, pp. S317-S323, 1997.

[28] M. Matsuishi and T. Endo, Fatigue of metals subjected to varying stress, *Proceedings of the Kyushu Branch of Japan Society of Mechanics Engineering*, Fukuoka, Japan (in Japanese), pp. 37-40, 1968.

[29] D. L. DuQuesnay, Applications of overload data to fatigue analysis and testing, *Application of Automation Technology in Fatigue and Fracture Testing and Analysis: Fourth Volume*, ASTM STP 1411, edited by Braun, A.A., McKeighan, P.C., Nicolson, A. M. & Lohr, R. D., ASTM, West Conshohocken USA, pp. 165-180, 2002.

## PROFILE

**S. Abdullah**
Department of Mechanical and Materials Engineering, Universiti Kebangsaan Malaysia, 43600 UKM Bangi, Selangor, Malaysia.